A neutron-spectroscopy study of two-dimensional hydrogen diffusion in the hydride halide $YBrH_{0.78}$

1994 J. Phys.: Condens. Matter 6 147

(http://iopscience.iop.org/0953-8984/6/1/016)

J. Phys.: Condens. Matter 6 (1994) 147–158. Printed in the UK

A neutron-spectroscopy study of two-dimensional hydrogen diffusion in the hydride halide $YBrH_{0.78}$

U Stuhr†, H Wipf†, R K Kremer‡, Hj Mattausch‡, A Simon‡ and J C Cook§

† Institut für Festkörperphysik, Technische Hochschule Darmstadt, D-64289 Darmstadt, Federal Republic of Germany

‡ Max-Planck-Institut für Festkörperforschung, D-70569 Stuttgart, Federal Republic of Germany

§ Institut Laue–Langevin, F-38042 Grenoble, France

Received 30 March 1993, in final form 23 September 1993

Abstract. The self-diffusion of H in the substoichiometric rare-earth hydride halide $YBrH_{0.78}$ was investigated by incoherent quasielastic neutron scattering. $YBrH_{0.78}$ exhibits a layered structure in which the H atoms occupy tetrahedral interstitial sites located in Y bilayers, which are sandwiched by Br bilayers. As this arrangement suppresses H transfer between different Y bilayers, the present study investigates an essentially two-dimensional H diffusion within a given Y bilayer. The self-diffusion coefficient of the H was determined to be between 750 and 900 K. At 900 K, its value is $D = (1.2 \pm 0.4) \times 10^{-6}$ cm^2 s^{-1}. The temperature dependence can be described by an Arrhenius relation with an activation energy $E = (0.48 \pm 0.12)$ eV. The momentum-transfer dependence of the measured spectra suggests the presence of noticeable correlation effects in the H diffusion.

1. Introduction

$YBrH_x$ belongs to a group of recently synthesized substoichiometric ($0.67 \leqslant x \leqslant 1$) hydride halides of the trivalent rare-earth metals [1, 2]. The compounds are metallic. A dominant characteristic is their layered crystal structure where close-packed bilayers of metal atoms are sandwiched by bilayers of the halogen atoms along the c axis (space group $R\bar{3}m$). The crystal structure of the investigated compound $YBrH_x$ is represented in figure 1. For this compound, the stacking sequence of the heavy atoms is AbcABcaBCabC where capital and lower-case letters stand for Br and Y, respectively (ZrCl structure) [2]. The H atoms occupy tetrahedral interstitial sites, surrounded by four metal atoms and located within the metal-atom bilayers. A full occupation of all interstitial sites corresponds to the maximum H concentration $x = 1$. The H sites within a given metal-atom bilayer form a two-dimensional hexagonal honeycomb sublattice as indicated in figure 2. In the case of $YBrH_x$, and for the H concentration $x = 0.78$ investigated in the present study, two nearest-neighbour sites of the H sublattice are separated by a distance $d \simeq 2.78$ Å [3]. Although the honeycomb sublattice is two dimensional, it is not completely planar because its sites are alternately shifted by a distance $\sim \alpha d$ parallel or antiparallel to the c-axis direction where the value of the factor α is 0.6105 [3] (for an ideal close-packed structure, the value of α is $1/\sqrt{3} = 0.5774$).

This paper reports the results of a quasielastic neutron-scattering study in which we investigated H self-diffusion in $YBrH_{0.78}$. A chief motivation for this study was the expectation that H transfer from the interstitial sites in one Y-atom bilayer to those in a neighbouring one will be strongly suppressed by the separating Br bilayers. This expectation

0953-8984/94/010147+12$07.50

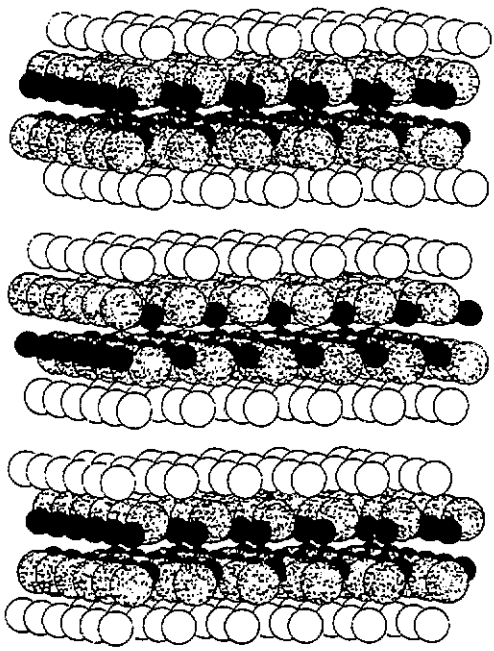

Figure 1. View of the crystal structure of the rare-earth hydride halide $YBrH_x$, showing the distinct layered structure of this compound. The open and shaded circles show the positions of the Br and Y atoms, respectively. The small full circles indicate the tetrahedral interstitial sites occupied by the H atoms. A full occupation of all sites corresponds to an H concentration $x = 1$.

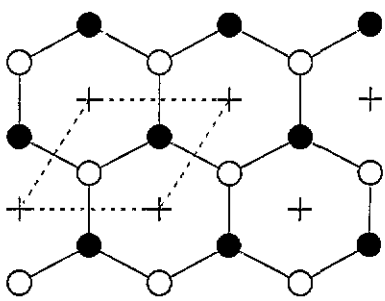

Figure 2. The two-dimensional honeycomb sublattice of the H atoms in the *ab* crystal plane. The full and open circles represent the tetrahedral sites occupied by the H. The sites indicated by full circles are shifted against the open ones in the *c*-axis direction by $\sim \alpha d$, where $d \simeq 2.78$ Å is the distance between two nearest-neighbour sites and the value of the factor α is 0.6105. The crosses show the positions of octahedral interstitial sites lying in the centre of six surrounding tetrahedral sites. The octahedral sites are discussed in connection with the diffusive paths of the H. The broken lines indicate the two-dimensional primitive unit cell.

is plausible because of the large van der Waals gap that exists between the Br atoms. Consequently, an H atom is virtually confined to the interstitial sites of a given Y bilayer resulting in a two-dimensional diffusion of H interstitials in the hexagonal honeycomb sublattice of figure 2.

A second aspect to consider in our study is that the high H site occupation probability $x = 0.78$ means that the appropriate description of the investigated diffusion process is that for a concentrated lattice gas. The correlations exhibited in the diffusion in concentrated lattice gases are the subject of continuous theoretical interest [4–16]. The two-dimensional diffusion case [10, 12, 13, 16] is particularly interesting because the influence of correlation effects rises with a lowering of the dimensionality. The specific case of diffusion on a two-dimensional honeycomb lattice, which exhibits the lowest possible coordination number $z = 3$, has been treated theoretically by Kutner [12]. The latter study reflects, therefore, precisely the situation found in our present experiments.

A final important aspect of our study is the structural similarity between the hydrogen positions in $YBrH_x$ and those in the dihydride phase of YH_x (CaF_2 structure [17, 18]) for which the H diffusion has been investigated recently by neutron spectroscopy [19–21]. In

both systems, H atoms are located on tetrahedral interstitial sites surrounded by four Y atoms. This structural similarity is underlined by the fact that the nearest-neighbour H separation in YH_x is only $\sim 7\%$ smaller than that in $YBrH_x$, and by the nearly identical values of the vibrational energies of the H atoms. These energies are ~ 0.117 eV (threefold degenerate) for YH_x [22,23] and ~ 0.121 eV and ~ 0.132 eV (twofold degenerate) for $YBrH_x$ [3]. However, we point out that the H diffusion processes in the two systems differ drastically, being three dimensional in YH_x and (practically) two dimensional in $YBrH_x$. A further difference is that a small fraction (below 10%) of the H interstitials in YH_x occupies octahedral sites (see [18,21,22] and references therein) whereas such an additional occupation of octahedral sites has not been observed for $YBrH_x$. Recent neutron-spectroscopy measurements [21] have demonstrated that the additional occupation of octahedral sites is essential for a correct description of the H diffusion behaviour in the dihydride YH_x. We shall see later that the octahedral sites are also likely to play an important rôle for H diffusion in the presently studied system $YBrH_x$ since a diffusion model in which the H atoms pass through octahedral sites in their diffusive jumps gives a better description of the data than a model that assumes only direct jumps between nearest-neighbour tetrahedral sites. Although the octahedral sites are involved in the diffusion process, their time-averaged occupation probability remains negligibly small.

The paper is organized as follows. In section 2, we give details of the sample preparation and of the neutron-scattering measurements. In section 3, we present two different jump-diffusion models for the honeycomb lattice shown in figure 2 and we derive for each the incoherent dynamic structure factor, i.e. the quantity that is experimentally determined. The experimental data are given in section 4. By comparing these data with the theoretical predictions of our two models, we obtain values for the self-diffusion coefficient and for the mean residence time of the H.

2. Sample preparation and experimental details

The $YBrH_{0.78}$ sample, in powdered form, was contained in the sealed annular space created between two cylindrically shaped quartz tubes. The dimensions were such that the sample shape was effectively a 50 mm long hollow cylinder of 16 mm outer diameter with a wall thickness of about 1 mm. At the experimental neutron wavelength, this sample geometry gives a neutron transmission of $\sim 60\%$ with about 35% of the scattering events originating from Bragg reflections. The $YBrH_{0.78}$ powder is sensitive to moisture and air. It was prepared according to standard procedures, which have been described in detail previously [24]. The crystal structure of the investigated powder was verified by x-ray diffraction, both before and after the neutron measurements, using a modified Guinier technique [25].

The quasielastic neutron spectra were measured using the backscattering instrument IN10 at the Institut Laue–Langevin in Grenoble (wavelength $\lambda = 6.275$ Å, energy resolution < 1.9 μeV). The angular positions of the analyser crystals allowed the investigation of seven different Q values in the range between 0.29 and 1.7 Å^{-1} (where $\hbar Q$ is the momentum transfer of the neutrons). The selected positions guaranteed that the analysers were not hit by Bragg reflections from the sample occurring at $Q = 0.651$ Å^{-1}, 1.301 Å^{-1} and above 1.919 Å^{-1}. During the measurements, the sample was kept in a temperature-regulated furnace (accuracy ± 10 K, stability ± 2 K). Spectra were taken at 750, 800, 850 and 900 K. Meaningful reference spectra of an H-free sample could not be taken since the compound $YBrH_x$ exists only for $x \geqslant 0.67$ [1,2].

3. Theoretical background

Information on the self-diffusion of the H atoms may be deduced by comparing the experimental results with model calculations for the incoherent dynamic structure factor $S(Q,\omega)$, where $\hbar Q$ and $\hbar\omega$ are the momentum and energy transfer, respectively, in the neutron-scattering process. In this section, we shall discuss the models for the two-dimensional H diffusion in the sublattice of the tetrahedral sites located in the *ab* crystal plane (see figure 2).

We consider first the limiting case of small Q, i.e. long-range H diffusion. In this case, the incoherent dynamic structure factor is Lorentzian [26,27],

$$S(Q,\omega) = (1/\pi)\Gamma/(\omega^2 + \Gamma^2) \tag{1}$$

where the width Γ is completely determined by the self-diffusion coefficient D of the H in the *ab* plane (diffusion in the *ab* plane is isotropic [28], and long-range diffusion in the *c*-axis direction does not exist). The width Γ can be written as

$$\Gamma = (Q_x^2 + Q_y^2)D = Q^2 D\cos^2\Theta \tag{2}$$

where D represents the self-diffusion coefficient in the *ab* plane, Q_x and Q_y are the Cartesian components of Q in the *ab* plane and Θ is the angle between Q and this plane.

Except for the above limit of small Q, the incoherent dynamic structure factor $S(Q,\omega)$ depends on the details of the hydrogen jump processes [26–31]. We shall consider two different models for the jump diffusion. The first model (I) assumes jumps only between nearest-neighbour tetrahedral sites. In this case, we need to define three different jump vectors $l_{1,i}$ given by

$$l_{1,1} = d\begin{pmatrix} \frac{\sqrt{3}\beta}{2} \\ \frac{-\beta}{2} \\ -\alpha \end{pmatrix} \qquad l_{1,2} = d\begin{pmatrix} 0 \\ \beta \\ -\alpha \end{pmatrix} \qquad l_{1,3} = d\begin{pmatrix} \frac{-\sqrt{3}\beta}{2} \\ \frac{-\beta}{2} \\ -\alpha \end{pmatrix} \tag{3}$$

where $d \simeq 2.78$ Å is the distance between two nearest-neighbour H sites, $\alpha = 0.6105$ (see section 1) and $\beta = \sqrt{1-\alpha^2} = 0.7920$. These jump vectors describe the jumps from tetrahedral sites indicated in figure 2 by full circles. The other jump vectors that exist in this model are given by the negative values of the vectors in (3). The second model (II) was motivated by the fact that H diffusion in the dihydride YH_x involves diffusive jumps passing through octahedral sites [21], as discussed in section 1. Model II assumes that the H jumps first to one of the three nearest-neighbour octahedral sites (step 1), and then *immediately* to one of the tetrahedral sites located around the octahedral site (step 2). The jumps of step 2 occur with equal probability to each of the accessible tetrahedral sites, if we neglect possible correlation effects (see later). The calculation of $S(Q,\omega)$ is simplified if we consider the two consecutive steps 1 and 2 as a single jump process taking place to one of the three nearest tetrahedral sites, to one of the six second-nearest sites or to one of the three third-nearest sites. The events in which the two consecutive steps lead back to the original site will not be counted as a jump process. We note further that, in the absence of correlation effects, the jump probability to one of the nearest sites is twice that to one of the more distant sites since jumps to the nearest sites can occur via two different octahedral sites. Considering again an H interstitial leaving one of the tetrahedral sites indicated by

full circles in figure 2, the jump vectors to the next-nearest sites are given by the three $l_{1,i}$ defined in (3). The six jump vectors $l_{2,i}$ to the second-nearest sites can be written as

$$l_{2,1} = d\begin{pmatrix}\sqrt{3}\beta\\0\\0\end{pmatrix} \qquad l_{2,2} = d\begin{pmatrix}\frac{\sqrt{3}\beta}{2}\\\frac{3}{2}\beta\\0\end{pmatrix} \qquad l_{2,3} = d\begin{pmatrix}\frac{-\sqrt{3}\beta}{2}\\\frac{3}{2}\beta\\0\end{pmatrix}$$

$$l_{2,4} = d\begin{pmatrix}-\sqrt{3}\beta\\0\\0\end{pmatrix} \qquad l_{2,5} = d\begin{pmatrix}\frac{-\sqrt{3}\beta}{2}\\-\frac{3}{2}\beta\\0\end{pmatrix} \qquad l_{2,6} = d\begin{pmatrix}\frac{\sqrt{3}\beta}{2}\\-\frac{3}{2}\beta\\0\end{pmatrix} \tag{4}$$

and the three jump vectors $l_{3,i}$ to the third-nearest-neighbour sites are

$$l_{3,1} = d\begin{pmatrix}\sqrt{3}\beta\\\beta\\-\alpha\end{pmatrix} \qquad l_{3,2} = d\begin{pmatrix}-\sqrt{3}\beta\\\beta\\-\alpha\end{pmatrix} \qquad l_{3,3} = d\begin{pmatrix}0\\2\beta\\-\alpha\end{pmatrix}. \tag{5}$$

For both models, the incoherent dynamic structure factor $S(Q,\omega)$ can be calculated by standard procedures [26,27,30,31] if we make the common approximation of neglecting any correlation effects in the sequence of the H jumps. In the following, we shall present the results of such a calculation. The possible consequences of correlation effects will be discussed later.

In the absence of correlation effects, the only additional quantity determining $S(Q,\omega)$ is the mean residence time τ of the H atoms on the tetrahedral sites. This holds for both models (I and II). The standard procedure for calculating $S(Q,\omega)$ yields a sum of two Lorentzian lines

$$S(Q,\omega) = \frac{1}{\pi}\sum_{j=1}^{2}\frac{w_j(Q)\Gamma_j(Q)}{\omega^2+\Gamma_j^2(Q)} \tag{6}$$

since a primitive unit cell of the honeycomb lattice has a basis of two lattice points. The weights $w_j(Q)$ and the widths $\Gamma_j(Q)$ of the two lines can be written as

$$w_1(Q) = \tfrac{1}{2}(1+\mathrm{Re}(K)/|K|) \qquad w_2(Q) = \tfrac{1}{2}(1-\mathrm{Re}(K)/|K|) \tag{7}$$

$$\Gamma_1(Q) = L-|K| \qquad \Gamma_2(Q) = L+|K| \tag{8}$$

where $\mathrm{Re}(K)$ represents the real part of K. The two quantities L and K differ for the two considered models. For model I, L and K are given by

$$L = \frac{1}{\tau} \qquad K = \frac{1}{3\tau}\sum_{i=1}^{3}\exp(\mathrm{i}Q\cdot l_{1,i}). \tag{9}$$

In the case of model II, the two quantities are

$$L = \frac{1}{15\tau}\left(15-\sum_{i=1}^{6}\exp(\mathrm{i}Q\cdot l_{2,i})\right) \qquad K = \frac{1}{15\tau}\left(2\sum_{i=1}^{3}\exp(\mathrm{i}Q\cdot l_{1,i})+\sum_{i=1}^{3}\exp(\mathrm{i}Q\cdot l_{3,i})\right). \tag{10}$$

The equations (6)–(10) determine completely $S(Q,\omega)$ for both models. We point out that the mean residence time τ is the only adjustable parameter for both models.

In the limit $Q \rightarrow 0$, the two expressions for $S(Q,\omega)$ in (1) and (6) become identical. This can also be seen from the fact that, according to (7), the weight factor $w_2(Q)$ in (6) tends to zero as Q tends to zero. In other words, $S(Q,\omega)$ can be described by a single Lorentzian line with a width Γ determined by the self-diffusion coefficient D (2). This allows the determination of the relation between D and τ of our two models. The calculation yields for model I

$$D = \tfrac{1}{6}d^2/\tau \tag{11}$$

and for model II

$$D = \tfrac{2}{5}d^2/\tau. \tag{12}$$

As we have already mentioned, the above calculations do not account for correlations in the sequence of the atomic jumps of a given H atom. In fact, we can distinguish two different types of correlation. Correlations of the first type arise at higher H concentrations due to interactions between different diffusing H atoms. This classical type of correlation was the subject of a large number of theoretical papers on concentrated lattice gases [4–16], cited in section 1. It has already been mentioned in this section that the influence of these correlations is larger for lower dimension [10]. The influence of these correlations is expected to be larger in the present two-dimensional situation than calculations for three-dimensional lattices show. The second type of correlation can occur even if only one single H atom occupies the sublattice of the tetrahedral sites. These correlations may result, for instance, from the fact that, within a short time after a jump, the H or the neighbouring lattice atoms, or both, may be in an energetically excited state so that the probability of an immediate second jump is increased. For a similar reason, we may also find a correlation in the direction of consecutive jumps (diffusion in a fixed volume is a special type of such a correlation). Correlation effects of the second type were discussed, for instance, in an analysis of neutron-scattering data for the diffusion of H in Nb [32,33].

In the limit $Q \rightarrow 0$, (1) and (2) still hold in the presence of correlation effects. However, the correlation modifies the relation between the self-diffusion coefficient D and the mean residence time τ, as given in (11) (model I) or (12) (model II). The influence of correlations can be considered by a multiplicative correlation factor f_{cor} on the right-hand side of (11) or (12). This factor depends on the H concentration x and, of course, on the diffusion mechanism. In the low-concentration limit $x \rightarrow 0$, f_{cor} has the value unity if we consider only correlations of type 1. For model I, we find $f_{cor} = \frac{1}{3}$ in the limit $x \rightarrow 1$ if we consider only correlations of type 1 and if we assume no H–H interactions other than the exclusion of double site occupancy [5,12]. Under the same assumptions, the value of f_{cor} can approximately be calculated over the entire concentration range $0 < x < 1$ [7,9].

It is finally important to point out that both types of correlation will modify $S(Q,\omega)$ in comparison with our model calculations above, except for the limit $Q \rightarrow 0$ where (1) and (2) still hold. This means, in particular, that possible inconsistencies between our model calculations and the experimental neutron spectra may be due to the fact that correlation effects were not appropriately accounted for.

4. Experimental results and discussion

Figure 3 shows quasielastic spectra measured at three temperatures and at two momentum transfers $\hbar Q$. The spectra show an increasing quasielastic linewidth with increasing

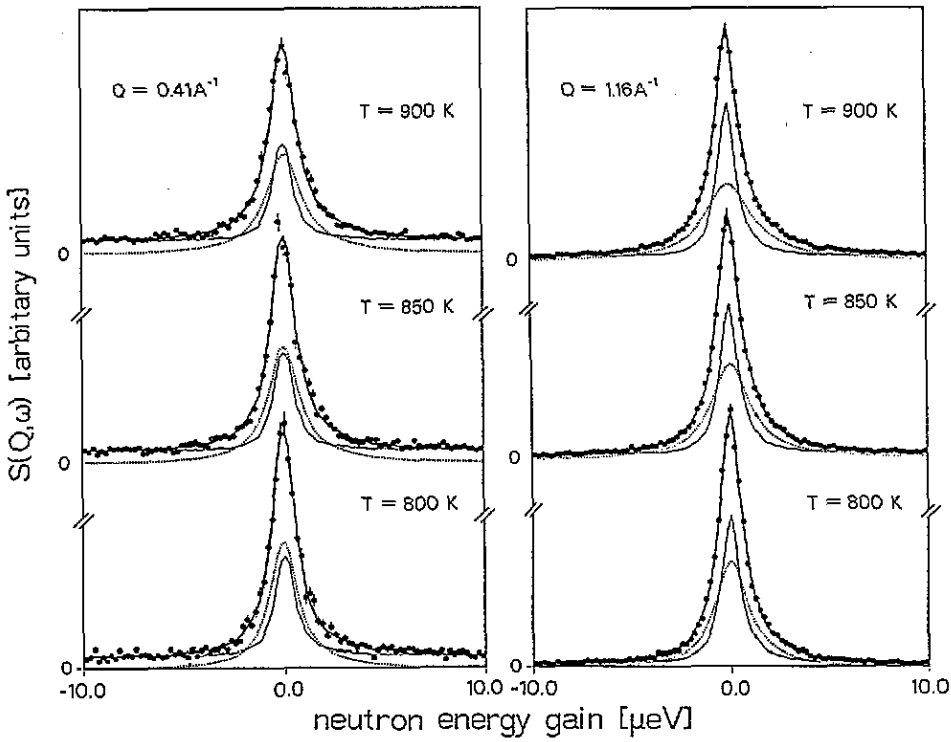

Figure 3. Quasielastic neutron spectra taken from the $YBrH_{0.78}$ sample at 800 K, 850 K and 900 K. The left-hand-side and right-hand-side plots show spectra for $Q = 0.41$ Å^{-1} and 1.16 Å^{-1}, respectively. The thick solid lines are curves fitted to the data according to our model II (see text). The thin solid lines are the elastic background (mainly from the quartz glass container) and the dots indicate the quasielastic scattering from the H as resulting from the fits.

temperature, as expected for a thermally activated diffusion process. The figure shows also that the linewidth is larger for the higher Q values.

For a quantitative analysis of our neutron data, the spectra were fitted to the two jump-diffusion models discussed in section 3. Because the samples were in a powdered form, the fits were performed using a numerical orientational average of the two respective incoherent dynamic structure factors $S(Q, \omega)$. The fits were carried out under consideration of the measured resolution function. Since meaningful reference spectra of an H-free sample could not be taken, the elastic background intensity from the sample and the quartz container was considered an adjustable parameter. A correction was made for double scattering using an analytic computer calculation which, in a previous neutron study [21], has been shown to provide similar results to the (slightly modified) Monte Carlo program DISCUS [34]. The correction requires an assumption for $S(Q, \omega)$ in the experimentally accessible Q range, which we chose to be the theoretical result for $S(Q, \omega)$ as predicted by either model I or II. The mean residence time τ was then determined self-consistently from the outcome of previous fits. The reduced chi square (χ^2_{red}) values [35] of the fits were essentially equally large for both models and varied within the range between 0.88 and 1.37.

The thick solid lines in figure 3 are curves fitted to the data there, calculated according to model II. The thin solid lines represent the elastic background, which is mainly caused by the quartz glass sample container. The dots indicate the quasielastic scattering intensity

as obtained from the fits.

In each fit, the relevant variable parameter was the mean residence time τ, which was determined independently for each spectrum. Figure 4 shows the jump rate $1/\tau$ and the self-diffusion coefficient D as functions of Q resulting from fits of model I to the 850 and 900 K spectra. The corresponding results for model II are given in figure 5. The self-diffusion coefficient D in figures 4 and 5 was calculated according to (11) for model I and (12) for model II.

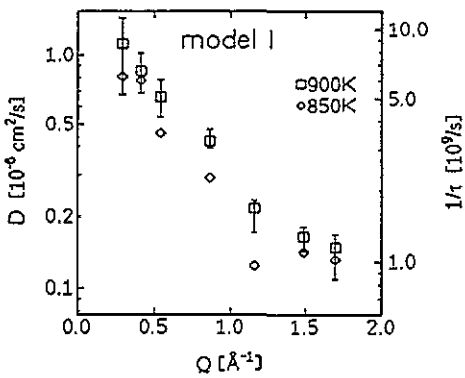

Figure 4. Fit results according to model I for the inverse mean residence time τ, or jump rate $1/\tau$, in a plot versus the Q value of the respective spectrum. The values of $1/\tau$ are presented at the right-hand ordinate. The analysed spectra were taken at 850 and 900 K. For reasons of perspicuity, error bars are only indicated for the 900 K data (the error bars for the 850 K data are generally slightly larger). The left-hand ordinate shows the value of the self-diffusion coefficient D as obtained from (11).

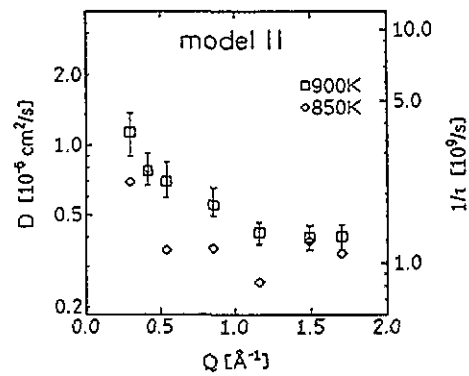

Figure 5. Fit results according to model II for the inverse mean residence time τ, or jump rate $1/\tau$, in a plot versus the Q value of the respective spectrum. The values of $1/\tau$ are presented at the right-hand ordinate. The analysed spectra were taken at 850 and 900 K. For reasons of perspicuity, error bars are only indicated for the 900 K data (the error bars for the 850 K data are generally slightly larger). The left-hand ordinate shows the value of the self-diffusion coefficient D as obtained from (12).

Figures 4 and 5 allow a serious test of the quality of the two theoretical models underlying our calculation of $S(Q, \omega)$ since, for a given temperature, the results for τ should be independent of Q if the correlation factor is considered to be Q independent. This criterion shows that both of the models cannot be entirely correct since τ varies with Q. However, it can be readily seen that model II provides a much better basis for an understanding of our data since the variation of τ does not exceed a factor of approximately three.

The Q dependence of τ as shown for model II in figure 5 may be the result of correlation effects that were not accounted for in our fits. However, this statement is certainly speculative since the presently available theoretical calculations for the influence of correlation effects on $S(Q, \omega)$ do not allow a reliable and quantitative prediction with respect to the present experimental data. This holds in particular for the calculations carried out for two-dimensional lattices [10, 12, 13, 16]. Some information may be derived from a Monte Carlo calculation [8] for a three-dimensional lattice gas in which the particles were assumed to be non-interacting except that double occupancy was forbidden. The calculation demonstrated that correlations of type 1 cause a decrease of the linewidth of $S(Q, \omega)$ which is more pronounced for higher Q values. This means that a data evaluation such as our present one, which did not consider correlation effects, would yield a lower jump rate

$1/\tau$ at higher Q, precisely as observed in figures 4 and 5. The same effect may result from correlations of type 2, for instance if an H atom has an increased jump probability immediately after it has completed a jump. Such a correlation favours the occurrence of sequences of several fast consecutive jumps which, in the absence of any spatial correlation effects, influences the Q dependence of the resulting spectra similarly to an increase of the average length of a single jump. How a model with longer jumps qualitatively changes our fit results for $1/\tau$ can be realized from a comparison between figures 4 and 5 since the main difference between the two models valid for these figures was the longer average jump lengths in the case of figure 5 (model II). The fact that the variation of $1/\tau$ with Q is smaller in figure 5 than in figure 4 makes it plausible that a correlation such as that discussed above, which in its consequences corresponds to larger jump lengths, could in principle explain the observed Q dependence of our fit results for $1/\tau$, particularly for the data in figure 5, which were determined with the help of model II.

The above discussion shows that correlation effects may in fact explain the Q dependence of τ that resulted from our fits. However, neither present theory nor the amount and quality of the present data allow a reliable discrimination between the large number of different correlation models that might apply. It is for this reason that we decided to restrict our analysis to two simple models that have only one variable parameter (i.e. $1/\tau$).

For the lowest investigated Q value ($Q = 0.29$ Å^{-1}), the incoherent dynamic structure factors $S(Q, \omega)$ of both models I and II are already well approximated by the limiting case of small Q as given in (1) and (2). This can be seen from (3)–(10) and it is also demonstrated by the fact that our two models yield, for our lowest Q, the same value for the self-diffusion coefficient D (see figures 4 and 5) although the jump distances of the two models are quite different. Accordingly, the D values determined for the lowest Q can be expected to represent an acceptable and model-independent approximate result for the self-diffusion coefficient of the H. Under consideration of this fact, we can conclude that, for a temperature of 900 K, the self-diffusion coefficient is given by $D = (1.2 \pm 0.4) \times 10^{-6}$ cm^2 s^{-1}. Again, we point out that, in the limit $Q \to 0$, $S(Q, \omega)$ is completely determined by the value of D according to (1) and (2), so D can be obtained unambiguously. The results derived for τ are, on the other hand, model dependent.

Figure 6 presents a compilation of our results for the self-diffusion coefficient D in a semilogarithmic plot versus reciprocal temperature. The figure needs an explanation. The value $D = 1.2 \times 10^{-6}$ cm^2 s^{-1} indicated for the temperature of 900 K is the result derived essentially model independently from the spectrum taken with our lowest Q (see also figures 4 and 5). The experimental error of $\pm 30\%$ for this result is not shown in figure 6. The results for the three other temperatures were derived for both of our models from the spectra measured at all the investigated Q. In this case, the indicated results were obtained from the ratio between the D value (or the inverse mean residence time $1/\tau$) determined from the spectra taken at the respective temperature and the spectra taken at 900 K. The ratios as obtained from spectra with different Q were averaged, and the resulting average was then normalized to the value of D at 900 K (the experimental errors in figure 6 represent the accuracy of the averaged ratios). The described procedure increases the experimental accuracy for the indicated D values since these values were determined from all our investigated Q rather than only for the lowest value $Q = 0.29$ Å^{-1}. The fact that the data analysis involved spectra with higher Q means in principle that the D values for the three lower temperatures are model dependent. However, this fact is not expected to cause any substantial inaccuracy since (i) the same model was applied to the spectra taken at different temperatures and (ii) our two models lead, within experimental accuracy, to identical results in figure 6.

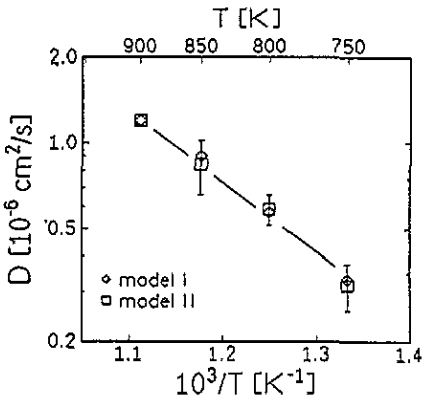

Figure 6. The self-diffusion coefficient D for two-dimensional H diffusion in $YBrH_{0.78}$ in a semilogarithmic plot versus reciprocal temperature. The data for the three lower temperatures were separately determined according to models I and II. Again for reasons of perspicuity, error bars are only shown for the results of model II. For more details, see the text.

In figure 6, the self-diffusion coefficient D can be described by an Arrhenius relation. The solid line in this figure yields an activation energy $E = (0.48 \pm 0.12)$ eV (the self-diffusion coefficient at 900 K is $D = (1.2 \pm 0.4) \times 10^{-6}$ cm^2 s^{-1}). In section 1, we mentioned the structural similarity between the presently investigated system and the dihydride $YH_{1.97}$, which makes it meaningful to compare the diffusion coefficients of the two systems. The comparison shows that, in the investigated temperature range, the self-diffusion coefficient of the H for two-dimensional diffusion in $YBrH_{0.78}$ is about 2.3 times smaller than that for three-dimensional diffusion in the dihydride $YH_{1.97}$, and that the present activation energy is considerably higher than that reported for $YH_{1.97}$ ($E \simeq 0.30$ eV) [21]. However, it was found that the self-diffusion coefficient in the system YH_x depends strongly on the H concentration x, exhibiting a drastic decrease with decreasing x. For the system YH_x, an identical occupation probability of the tetrahedral sites like that of the present hydride halide $YBrH_{0.78}$ corresponds to a concentration $x \simeq 1.56$, so the differences in the diffusion coefficients may in fact be much smaller for comparable occupation probabilities.

Finally it seems interesting to compare the present neutron-spectroscopy results for the self-diffusion coefficient of the H with nuclear-magnetic-resonance data reported for H nuclei in the related layered systems $ZrBrH_x$ and $ZrClH_x$ [36, 37]. The heavy atoms in these two systems exhibit the same crystal structure (space group $R\bar{3}m$) as the presently investigated rare-earth compound $YBrH_x$, except for a possibly different stacking sequence, and it is generally assumed that the H atoms also occupy—at least predominantly—tetrahedral interstitial sites that are located in the Zr bilayers. One of the nuclear-magnetic-resonance studies above reports activation energies for H diffusion, derived from linewidth data taken below $\sim$ 400 K [36]. Depending on the system, the H concentration and the temperature range, the activation energies that were found vary between 0.11 and 0.98 eV. The large variation in the values of the activation energies makes a comparison with the present result difficult, in particular since this variation may also reflect ordering processes of the H atoms. The second study [37] reports correlation times τ_{cor} in the range of several 10^{-4} s for the motion of the H at room temperature, derived from the measured values of the transverse relaxation time and the second moment. These correlation times can be compared with mean residence times τ derived from the present neutron study. A room-temperature extrapolation (293 K) of the neutron data in figure 6 leads to a self-diffusion

coefficient $D \simeq 3.2 \times 10^{-12}$ cm^2 s^{-1} yielding, for models I and II, mean residence times $\tau = 4 \times 10^{-5}$ s and $\tau = 1 \times 10^{-4}$ s according to (11) and (12), respectively. The values for τ differ by less than a factor of ten from the correlation times τ_{cor} of [13], which indicates a surprisingly similar two-dimensional diffusion behaviour of the H in the three layered compounds $YBrH_x$, $ZrBrH_x$ and $ZrClH_x$.

5. Conclusions

We performed a neutron-spectroscopy study investigating two-dimensional H diffusion in the hydride halide $YBrH_{0.78}$. The self-diffusion coefficient of the H was determined in the temperature range between 750 and 900 K. The variation of the neutron spectra with momentum transfer suggests the presence of noticeable correlation effects.

Acknowledgments

This work was financially supported by the Bundesministerium für Forschung und Technologie. We thank R Eger and C Hochrathner for their help in the sample preparation.

References

[1] Simon A, Mattausch Hj, Miller G J, Bauhofer W and Kremer R K 1991 *Handbook on Physics and Chemistry of Rare Earths* vol 15, ed K A Gschneidner Jr and L Eyring (Amsterdam: North-Holland) p 191
[2] Mattausch Hj, Eger R, Corbett J D and Simon A 1992 *Z. Anorg. (Allg.) Chem.* **616** 157
[3] Kremer R K, Cockcroft J K, Mattausch Hj, Simon A and Kearley G J 1993 to be published
[4] Bardeen J and Herring C 1952 *Imperfections in Nearly Perfect Crystals* ed W Shockley (New York: Wiley) p 261
[5] Le Claire A D 1970 *Physical Chemistry* vol 10, ed W Jost (New York: Academic) p 261
[6] Ross D K and Wilson D L T 1978 *Neutron Inelastic Scattering 1977, Proc. IAEA* vol 2 (Vienna: International Atomic Energy Agency) p 383
[7] Nakasato K and Kitahara K 1980 *Prog. Theor. Phys.* **64** 2261
[8] Kehr K W, Kutner R and Binder K 1981 *Phys. Rev.* B **23** 4931
[9] Tahir-Kheli R A and Elliott R J 1983 *Phys. Rev.* B **27** 844
[10] Tahir-Kheli R A 1983 *Phys. Rev.* B **27** 6072
[11] Koiwa M and Ishioka S 1983 *Phil. Mag.* A **47** 927
[12] Kutner R 1985 *J. Phys. C: Solid State Phys.* **18** 6323
[13] Kehr K W and Binder K 1987 *Applications of the Monte-Carlo Method in Statistical Physics (Topics in Current Physics 36)* ed K Binder (Berlin: Springer) p 181
[14] Faux D A and Ross D K 1987 *J. Phys. C: Solid State Phys.* **20** 1441
[15] Ross D K 1989 *Z. Phys. Chem, NF* **164** 897
[16] Kutner R and Kehr K W 1990 *Phys. Rev.* B **41** 2784
[17] Mueller W M, Blackledge J P and Libowitz G G (ed) 1968 *Metal Hydrides* (New York: Academic)
[18] Khatamian D and Manchester F D 1988 *Bull. Alloy Phase Diagrams* **9** 252
[19] Stuhr U, Schlereth M, Steinbinder D, Wipf H, Frick B and Magerl A 1989 *Z. Phys. Chem., NF* **164** 929
[20] Barnfather K J, Seymour E F W, Styles G A, Dianoux A-J, Barnes R G and Torgeson D R 1989 *Z. Phys. Chem., NF* **164** 935
[21] Stuhr U, Steinbinder D, Wipf H and Frick B 1992 *Europhys. Lett.* **20** 117
[22] Goldstone J A, Eckert J, Richards P M and Venturini E L 1984 *Solid State Commun.* **49** 475
[23] Semenov V A and Lisichkin Yu V 1985 *Sov. Phys.–Solid State* **27** 158
[24] Mattausch H, Schramm W, Eger R and Simon A 1985 *Z. Anorg. (Allg.) Chem.* **530** 43
[25] Simon A 1970 *J. Appl. Crystallogr.* **3** 11
[26] Springer T 1972 *Springer Tracts in Modern Physics* vol 64, ed G Höhler (Berlin: Springer)
[27] Bée M 1988 *Quasielastic Neutron Scattering* (Bristol: Hilger)

[28] Nye J F 1976 *Physical Properties of Crystals* (Oxford: Clarendon)
[29] Chudley C T and Elliott R J 1961 *Proc. Phys. Soc.* **77** 353
[30] Rowe J M, Sköld K, Flotow H E and Rush J J 1971 *J. Phys. Chem. Solids* **32** 41
[31] Anderson I S, Heidemann A, Bonnet J E, Ross D K, Wilson S K P and McKergow M W 1984 *J. Less-Common Met.* **101** 405
[32] Lottner V, Haus J W, Heim A and Kehr K W 1979 *J. Phys. Chem. Solids* **40** 557
[33] Lottner V, Heim A and Springer T 1979 *Z. Phys.* B **32** 157
[34] Johnson M W 1974 *Atomic Energy Research Establishment, Harwell Report* AERE-R7682
[35] Bevington P R 1969 *Data Reduction and Error Analysis for the Physical Sciences* (New York McGraw-Hill)
[36] Hwang T Y, Torgeson D R and Barnes R G 1978 *Phys. Lett.* **66A** 137
[37] Murphy P D and Gerstein B C 1979 *J. Chem. Phys.* **70** 4552